

Possible effects of RF field near ICRF antenna on density control during long pulse discharge in LHD

K. Saito ^{a,*}, R. Kumazawa ^a, T. Mutoh ^a, T. Seki ^a, T. Watari ^a, Y. Nakamura ^a,
M. Sakamoto ^b, N. Noda ^a, T. Watanabe ^a, M. Shoji ^a, S. Masuzaki ^a,
S. Morita ^a, M. Goto ^a, Y. Torii ^c, N. Takeuchi ^d, F. Shimpō ^a, G. Nomura ^a,
M. Yokota ^a, A. Kato ^a, Y. Zhao ^e, LHD Experimental Group

^a National Institute for Fusion Science, 322-6 Oroshi, Toki 509-5292, Japan

^b Research Institute for Applied Mechanics, Kyushu University, Kasugai 816-8580, Japan

^c Institute of Advanced Energy, Kyoto University, Uji 611-0011, Japan

^d Faculty of Engineering, Nagoya University, Nagoya, 464-8603, Japan

^e Institute of Plasma Physics, Chinese Academy of Science, Hefei 230031, People's Republic of China

Abstract

In the large helical device (LHD), the plasma duration time was extended up to 150 s by ion cyclotron range of frequencies (ICRF) heating. Time-integrated total input power reached 71 MJ. However, this discharge terminated due to radiation collapse accompanied by an increase of electron density. The temperature of the divertor plates and the intensity of H_α were locally increased in the same toroidal section, near the ICRF antenna. One of the possible causes of the increase of radiation power is an outgassing from the divertor plates that were heated by particles accelerated in the cyclotron resonance layer near the antenna. Another possible cause is the outgassing from the ICRF antenna itself due to a temperature increase of the ICRF antenna owing to high-energy particles, or the formation of an RF (radio frequency) sheath.

© 2004 Elsevier B.V. All rights reserved.

PACS: 52.40.Fd; 52.40.Hf; 52.50.-b; 52.50.Gj

Keywords: ICRF; LHD; Outgassing; RF; Steady state

1. Introduction

Long pulse operation has been conducted in various fusion devices [1–3]. Steady state operation is one of the main objectives of the large helical device (LHD) [4,5].

The LHD is a $l = 2$, and $m = 10$ helical device, where l and m are poloidal and toroidal mode numbers, respectively. It has inner and outer ports numbered 1, 2, ..., 10 and upper and lower ports numbered 1.5, 2.5, ..., 10.5. At the toroidal section of inner and outer ports, plasma is horizontally elongated and at the toroidal section of upper and lower ports, plasma is vertically elongated. The LHD is suitable for steady state operation because it is possible to operate without plasma current.

* Corresponding author.

E-mail address: saito@nifs.ac.jp (K. Saito).

Ion cyclotron range of frequencies (ICRF) heating is one of the methods used for the plasma heating. For the ICRF heating, three pairs of loop antennas [6] are installed in the LHD. The antenna current is set perpendicular to the toroidal direction in order to launch the fast wave. The RF (radio frequency) power is fed into the ICRF antennas from the upper and lower ports of the LHD. Each of the antennas is 46 cm wide, 60 cm long, and 17 cm thick. Graphite side protectors are attached on both sides of each antenna to protect it against the plasma heat load. The antennas have twisted shapes to fit the last closed flux surface (LCFS) of the helical plasma, and are movable by 16 cm in the radial direction to allow for adjustment in the distance between the antennas and LCFS. The straps, back plates, and Faraday shields are water cooled for steady-state operation. There are several heating scenarios using the ICRF. Minority ion heating, mode conversion heating, and second harmonic heating have been mainly conducted in the LHD. A stored energy of 240 kJ was obtained by the minority ion heating with the power of 2.3 MW [7], and the steady state experiment was conducted with minority ion heating. With minority ions (resonant ions) and majority ions, a strong left-hand polarized RF field that accelerates resonant particles emerges near the ion cyclotron resonance layer. In the LHD, helium is used as the majority ion and hydrogen as the minority ion. A high heating efficiency (absorbed power/injected power) of 80% was obtained when the frequency f was 38.47 MHz, and the magnetic field strength on axis B_{ax} was 2.75 T [8]. Then, as shown in

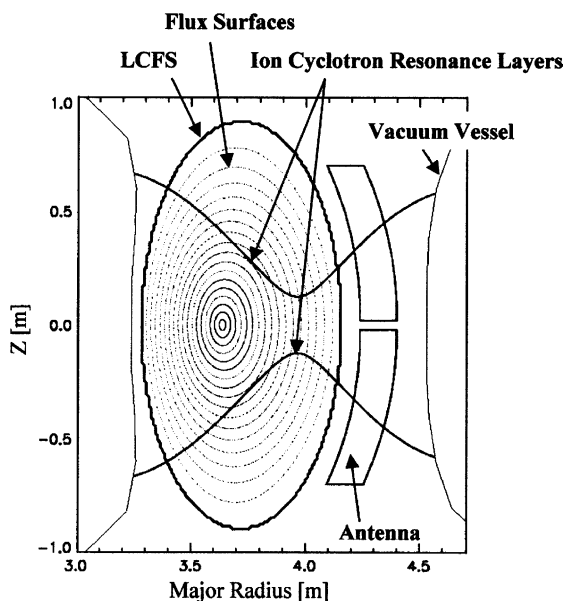


Fig. 1. Ion cyclotron resonance layers in the minority heating scenario. Frequency is 38.47 MHz, and the magnetic field strength on axis is 2.75 T.

Fig. 1, the ion cyclotron resonance layers were located near the saddle point, where the gradient of magnetic field strength was null, and the ion cyclotron resonance layers crossed the ICRF antenna.

Long pulse experiments have been conducted previously in the LHD. A plasma with a line averaged electron density of $1.5 \times 10^{19} \text{ m}^{-3}$ and a central electron temperature of 1.8 keV was sustained for 80 s by the neutral beam injection (NBI) heating with a heating power of 0.5 MW [9], and the electron density of $0.8 \times 10^{19} \text{ m}^{-3}$ and electron temperature of 1.2 keV was sustained for 120 s by the ICRF heating with a heating power of 0.4 MW without a plasma collapse [7].

In Section 2, the experimental results of a 150 s discharge by the ICRF heating are described. In Section 3, the causes of plasma collapse at 150 s are mentioned. Conclusion and future plans for steady state operation are mentioned in Section 4.

2. Steady state ICRF experiment

The duration time of plasma sustainment by an ICRF minority heating was extended up to 150 s [10]. Fig. 2 shows the time evolution of plasma parameters. A pair of loop antennas at the toroidal section of No. 3.5 port where the plasma was vertically elongated was used in the experiment, and net injected power was 500 kW. Time-integrated total input power reached 71 MJ. Electron temperature on axis T_{e0} and ion temperature on axis T_{i0} were 2 keV, and the line averaged electron density \bar{n}_e was $0.6 \times 10^{19} \text{ m}^{-3}$. However, this 150 s discharge was terminated by the collapse of the plasma due to the increase of radiation power P_{rad} owing to an outgassing. Intensities of CIII, OV, H, and HeI were increased. Only the intensity of H_α measured at the No. 3 outer port normalized by the line averaged electron density increased drastically. Therefore outgassing was mainly attributed to hydrogen. The maximum wall temperature T_{wall} which was measured by thermocouples increased only by 3 °C, but the maximum temperature of the graphite divertor plates T_{div} which was also measured by thermocouples reached 400 °C, which was higher than the baking temperature of 95 °C. As shown in Fig. 3(a) and (b), the divertor plate temperature and the H_α intensity were locally increased in the same toroidal section near the ICRF antenna.

3. Possible causes of plasma collapse

There are some candidate explanations for the plasma collapse. An outgassing due to the heat load from plasma to the ICRF antenna was ruled out. The distance between LCFS and the ICRF antenna was 7 cm. For this location of the antenna, the heat load from the

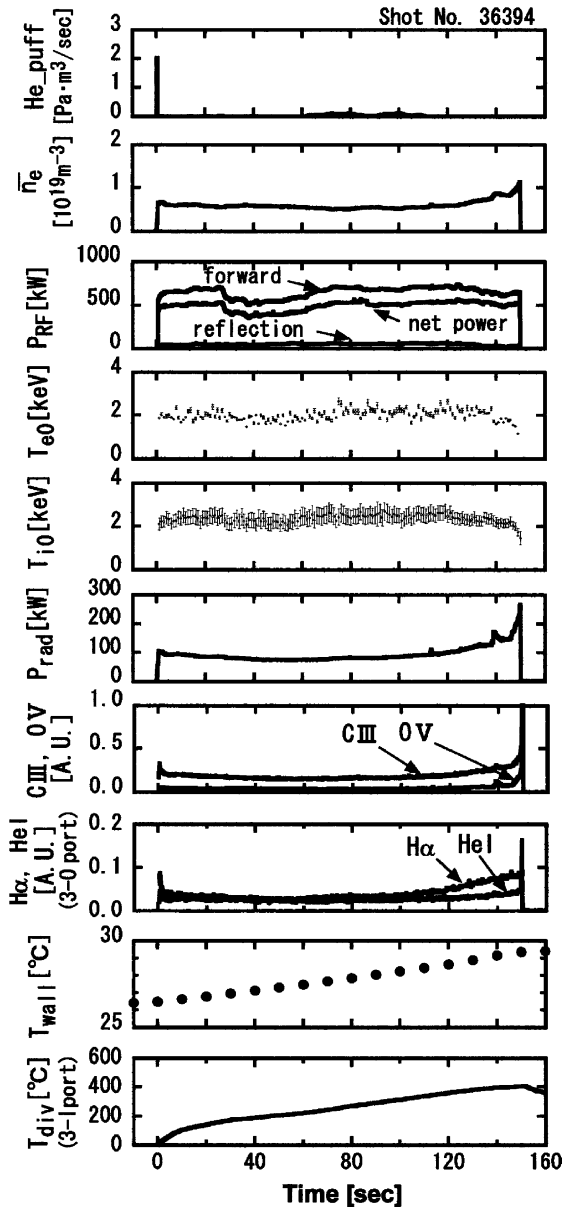


Fig. 2. Time evolution of plasma parameters in the long pulse discharge of 150 s.

plasma is negligible because the connection length of the magnetic field line from the ICRF antenna to the wall in this location is only a few meters and plasma particles cannot be confined.

One of the possible causes of the increase of radiation power was an outgassing from the graphite divertor plates, which were heated due to a direct loss of the high-energy ions accelerated at the peripheral cyclotron resonance layer just in front of the ICRF antenna. Orbits of resonant particles with various initial pitch angles

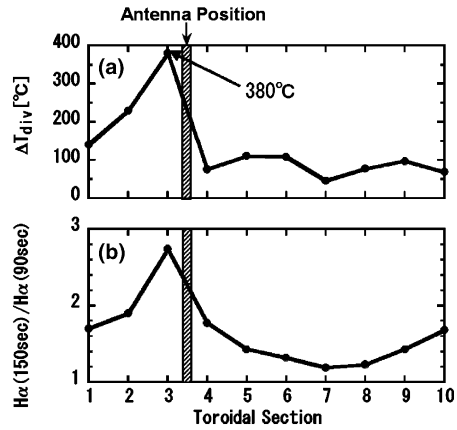


Fig. 3. (a) Temperature rise in divertor plates located on the inner side of the torus at the end of 150 s discharge. The temperature at the No. 3 toroidal section increased by 380 °C and reached 400 °C. (b) The ratio of H α intensity at 150 s and 90 s detected at the outer ports.

were calculated [11]. Initial positions of resonant particles were located on the ion cyclotron resonance layer outside of the LCFS near the ICRF antenna. The strength of RF field was deduced from the calculation of a one-dimensional wave equation [12]. In this calculation, the divertor plates were not included. However, the hit points on the vacuum vessel were along the divertor plates. Fig. 4 shows the relation between the terminal energy on the vacuum vessel and the starting position. Even in the unconfined plasma region, the terminal energy reaches several keV, and it increases with the distance from the ICRF antenna because the particles which start from the outer positions immediately escape to the divertor plates, but the particles which start from the inner

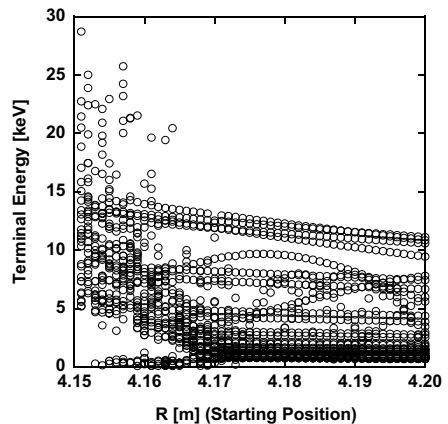


Fig. 4. The terminal energy on the vacuum vessel. It can reach several keV.

positions circulate the torus many times and are accelerated every time they cross the toroidal section of the antenna and gain high energy. From this calculation it was found that some of the particles accelerated at the resonance layer in front of the antennas hit the vertically installed divertor plate located at the No. 2.5 lower port. This was observed as a hot spot, which was recognized immediately after the start of the ICRF heating by a CCD camera but was not observed in the NBI plasma. Fig. 5 shows the calculated distribution of the heat load that is the summation of the terminal energy on the vacuum vessel in one toroidal section. This distribution is similar to that of the temperature rise on divertor plates and the increase of H_α intensity shown in Fig. 3(a) and (b), respectively. Therefore, the heat load by the high-energy particles accelerated by RF field near the ICRF antenna is one possible explanation for the outgassing in the long pulse experiment.

Another possible cause of the increase of radiation power is an outgassing due to a temperature increase in the ICRF antenna itself. High-energy particles accelerated inside the ICRF antenna can increase the antenna temperature because they hit the graphite side protectors with an energy of several keV, and the heat load due to the RF sheath potential also increases the temperature. A magnetic field B is induced by the antenna current I in the tip of the ICRF antenna as shown in Fig. 6. This magnetic field induces RF voltage between the graphite side protector and the tip of the strap. Therefore, a RF sheath is formed [13] and the heat load by ion injection can be calculated using the following equation:

$$Q = 0.02n_e\sqrt{T_i + T_e}f\sqrt{P_{in}/R}, \quad (1)$$

where Q is the heat load at the tip of antenna in MW/m^2 , n_e is the electron density in 10^{18} m^{-3} , and T_i , T_e are ion

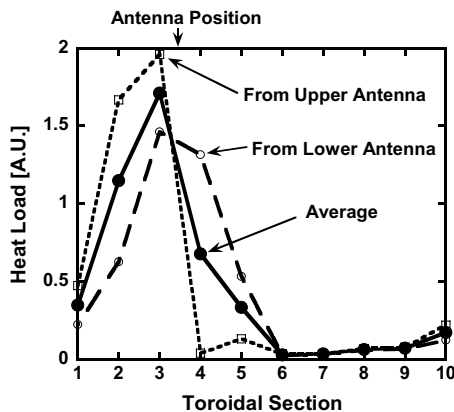


Fig. 5. A calculated distribution of the heat load by the high-energy particles. The No. 3 toroidal section has the largest heat load.

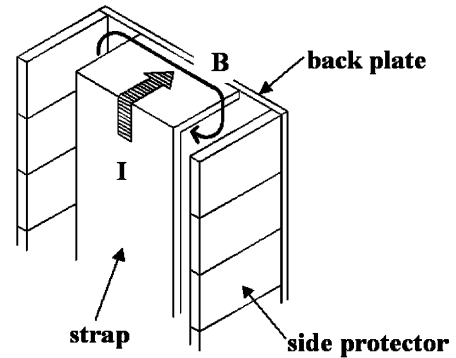


Fig. 6. Schematic view of the tip of the ICRF antenna. The antenna current I on the strap produces magnetic field B around the strap. It induces voltage between the strap and the side protector.

and electron temperature in eV, respectively. f is the frequency in MHz, P_{in} is the input power in MW, and R is the loading resistance of antenna in Ω . The coefficient 0.02 was determined using the dimensions of the ICRF antenna. In the long pulse experiment f was 38.47 MHz, P_{in} was 0.25 MW, R was 2.5 Ω , but T_i , T_e , and n_e were unknown. If T_i and T_e are 100 eV and n_e is $1 \times 10^{18} \text{ m}^{-3}$, then Q is $3.4 \text{ MW}/\text{m}^2$. Therefore, the existence of the thin plasma inside the antenna would increase the temperature of the ICRF antenna. At the present time we are not instrumented to detect the temperature in the experiment.

4. Conclusion and future plans for steady state operation

The duration time and total input energy reached 150 s and 71 MJ, respectively, using ICRF minority heating. But the plasma was collapsed by the increase of radiation power due to outgassing. It is thought that the outgassing in this long pulse experiment was induced by a local temperature increase of the divertor plates or the antenna itself.

On-axis minority heating, and mode conversion heating are candidates for steady state operation because the ion cyclotron resonance layer does not exist just in front of the antenna where the RF field is strong. Therefore, local heating of the divertor plates shown in Fig. 3(a) will be avoided. The particles of the edge plasma are not accelerated by second harmonic heating because of the weak finite Larmor radius effect in the low temperature edge plasma. Therefore, the second harmonic heating scenario is another candidate for steady state operation. An infrared camera will be installed on the LHD to measure the temperature of the ICRF antenna in the next experimental campaign and to help to determine the optimal condition for the antenna temperature.

References

- [1] H. Zushi et al., Nucl. Fus. 41 (2001) 1483.
- [2] J. Paméla et al., Nucl. Fus. 43 (2003) 1540.
- [3] D. van Houtte et al., Nucl. Fus. 44 (2004) L11.
- [4] M. Fujiwara et al., J. Fus. Eng. 15 (1996) 7.
- [5] O. Motojima et al., Nucl. Fus. 43 (2003) 1674.
- [6] T. Mutoh et al., J. Plasma Fus. Res. Series 1 (1998) 334.
- [7] T. Seki et al., Proceedings of 14th Topics Conference on RF Power in Plasmas 595 (2001) 67.
- [8] K. Saito et al., Nucl. Fus. 41 (2001) 1021.
- [9] N. Noda et al., Nucl. Fus. 41 (2001) 779.
- [10] K. Saito et al., Proceedings of 15th Topics Conference on RF Power in Plasmas 694 (2003) 58.
- [11] Y. Matsumoto, T. Nagaura, S. Oikawa, T. Watanabe, Jpn. J. Appl. Phys. 43 (2004) 332.
- [12] A. Bers, L.P. Harten, A. Ram, Proceedings of 4th Topics Conference on RF Plasma Heating (1981) A16.
- [13] D.A. D'Ippolito, J.R. Myra, Phys. Plasmas 3 (1996) 420.